encit 2020

ABCM Associação Brasileira de Engenharia e Ciências Mecânicas

18th Brazilian Congress of Thermal Sciences and Engineering
November 16-20, 2020 (Online)

ENC-2020-0407
CFD ANALYSIS OF THE SWIRL NUMBER INFLUENCE IN THE FORMATION OF RECIRCULATION ZONES IN A COMBUSTOR FOR GAS TURBINE APPLICATION

Arthur França Martins
Diego Paes de Andrade Peña
Dener Silva de Almeida
Av. dos Portugueses, 1966 - Vila Bacanga, São Luís - MA, 65080-805
arthur.franca@discente.ufma.br
diego.pena@ufma.br
dener.almeida@ufma.br

Resumo. *Gas turbines are widely used for power generation and aeronautical propulsion. These equipments make use of swirler devices to obtain recirculation structures in the flow by adding a tangential velocity component. The present work aims to, numerically, analyze combustion instabilities, obtained experimentally through a laboratorial scale gas turbine combustor. Such analysis consists in creating and simulating a CAD model via CFD, to better understand the recirculation structures formed within it, as well as the factors that led to combustion instabilities generation in the studied chamber. Results indicate that, mostly, high swirl numbers lead to more homogenous recirculation structures, which are preponderant to attenuate the pressure oscillations.*

Keywords: *gas turbine, instability, swirler, numerical simulation.*

1. INTRODUCTION

The gas turbine is regarded as one of the greatest inventions of the 20th century, having its development started before the World War I; however, its application was meant to energy generation. These equipments were little competitive due to their low power and thermal efficiency. At the start of the 21st century, gas turbines were able to output up to 500 MW with a thermal efficiency of above 40%, and became largely employed in energy generation. Aircraft propulsion oriented turbine development started during the World War II, aiming to build high velocity military grade airships. It is known that the first engines had shown to be short-lived, unreliable and inefficient, which resulted in civil aircraft applications only in the 50's (SARAVANAMUTTOO *et al.*, 2008). Traditionally, gas turbines employ combustors which use diffusion flames due to their reliable performance and reasonable stability (HUANG; YANG, 2009). In this kind of configuration, reagents are mixed within the combustion chamber and the reaction occurs next to stoichiometric conditions (minimum amount of oxidant to a full combustion), obtaining as such, the formation of a stable flame at the combustor's primary combustion zone. Afterwards, additional air amounts are injected into the remaining chamber combustion zones aiming an adequate temperature to the turbine blades. However, due to the reaction occurring at the edge of stoichiometry, this type of combustor is characterized by a high production of NOx levels (SUNG, 2007).

In order to reduce the production of such pollutants the concept of LP (*Lean Premixed*) is largely used. LP chambers operate with a lean mixture, as to reduce the emission of nitrogen oxides. These chambers premix fuel and oxidant before ignition, avoiding then the formation of zones with stoichiometric mixtures and consequentially, high-temperature zones that form NOx (LEFEBVRE; BALLAL, 2010). Yet according to Richards and Janus (1998) and Lefebvre and Ballal (2010), such chambers are more susceptible to combustion instabilities due to their functioning process.

Combustion instabilities are, according to Lieuwen (2006), high amplitude oscillations, presenting one or more acoustic modes that occur in the combustor. These instabilities appear in energy generation processes, combustion, propulsion, boilers and heating systems, and industrial furnaces. In general, those instabilities are spontaneous excitations created by an operational loop between a combustion process and one of the combustor's natural acoustic mode, and as such it is the very resonance between the combustion processes own acoustic mode and the combustors common acoustic mode (LIEUWEN; YANG, 2005). To Lang and Vortmeyer (1987) in order to sustain pressure oscillations, it is necessary the addition of heat, as the oscillations need to be synchronized (in phase). As such, self-sustained oscillations in the combustion chamber are the result of more than one oscillation frequency in the chamber

and that different forms of overlapping occur dependent of different frequency amplitudes. Generally, the occurrence of instabilities incurs in problems such as thermal and mechanical fatigue, as well as efficiency reduction and emission increase in gas turbine engines. (KHEIRKHAH et al., 2017).

Another potential concept to reduce NOx, CO and UHC emission, is the RQL (*Rich-Quench-Lean*) which is based in combustion occurring in two different zones, bridged by a quick cooling through air insertion (INGENITO *et al*, 2015). The first zone is characterized by a rich burn (equivalence ratio of typically 1.2, 1.6 and even 1.8 in some arrangements), while the second zone shows lean burn (equivalence ratio between 0.5 and 0.7). Combustion ~~by~~ products, which still contain a large amount of fuel, must flow from the rich burn zone and undergo quick cooling on their way to the lean burn zone, in order to avoid NOx generation. Nevertheless, an extremely fast and efficient cooling system is hard to implement, rendering this system's operation harder.

In light of these circumstances, the airflow pattern in the primary zone is of utmost importance, not only to aerodynamic stability and flame stability, but also to the gas turbine performance. Different flow patterns are employed but among them, it is commonly seen the use of flows with a tangential velocity component (*Swirl Flow*) originated through devices known as *Swirlers* to control intensity, size and shape of a flame in a gas turbine. This device is largely utilized in gas turbines combustion due to its capacity of generating recirculation zones. Flows with a high swirl number (S'=0.6), which is a dimensionless number that quantifies the recirculation zone's intensity, produce a radial pressure gradient, sustaining the air at the combustor's walls. With the diminishing of the centrifugal force, air moves to the chamber center, and forms CTRZ (Central Toroidal Recirculation Zone). Furthermore, it is possible the occurrence of CRZ (Cone Recirculation Zone) whenever a sudden expansion in the combustor (GUPTA *et al*., 1984).

The use of swirler in conjunction with high air velocitys may lead to formation of structures denominated Vortex Breakdown (VB). Leibovich (1978) characterizes said structure as a disturbance resulting in an internal stagnation point, followed by a reverse flow in an extension region that is axial to the flow, allowing as such the flame's stabilization. In turn, Precessing Vortex Core (PVC) develops when a vortex core spins around the symmetry axis at a well-defined frequency. This phenomenon relates to Vortex Breakdown and flows with high Reynolds number, localized at the edge of the reverse flow zone. (HUANG, YANG, 2009).

The concept presented in this paper was proposed by Almeida (2007, 2011). In figure 1 RQL and LP concepts are utilized, though without staged air addition as in RQL combustors, and without premixing of reagents inherent to LP combustion chambers, employing a swirler device as a flame anchor. This way it is possible to minimize operational problems characteristic to said systems and the emission of pollutants is reduced through control of the process dynamic, which in turn provides advantages over conventional methods.

According to Almeida (2007), in this configuration the fuel (natural vehicular gas) and air are directly injected in a primary chamber, in which fuel is injected through a central nozzle and the air that participates in the global process of combustion going through the swirler. Due to the swirler only a small fraction of airflow interacts with the fuel jet that occupies the chamber's central zone (Rich Zone). The air that doesn't participate in this first combustion zone forms a protective film on the chamber walls (Film Cooling). By the end of the primary zone, there is an expansion in the chamber diameter and consequentially the spinning airflow tends to expand radially, creating a low pressure zone at the chamber's central region. This zone originates an intense recirculation zone by mixing the remaining air with the combustion products from the primary zone (Quench effect). This recirculating zone provides favorable conditions to a lean homogenous combustion mixture though intense mixture between reagents.

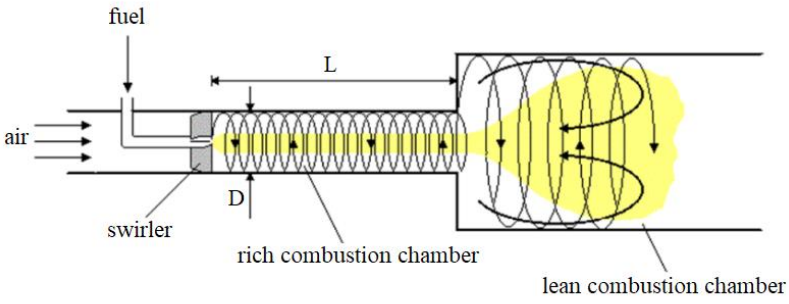

Figure 1. Flow diagram along a combustion chamber
Available in Almeida (2007)

Besides the NOx reduction provided by this experimental build, it is observed that to some operation conditions the combustion acoustic instabilities. As such, the present study consists in analyze, numerically the experimentally obtained results by Almeida (2007, 2011) in order to better comprehend the flow field with the formed recirculation structures and their influence over the generation of instabilities in an environment without chemical reactions.

2. METHODOLOGY

According to Almeida (2007), the primary zone has a variable length, that is L = 10, 20 and 30 cm, and fixed diameter D_c = 10 cm. In turn, the secondary zone has L_s = 50 cm and diameter equal to twice the primary chamber's own diameter (20 cm) and a nozzle at is end, with a starting and ending diameter of respectively 20 and 10 cm. the inclination of the nozzle's wall is β = 56,31°. The entire chamber was built in stainless steel.

The dimensionless parameters that control the flow dynamics are the jet fuel Reynolds Number (Re_{comb}) that characterizes the turbulence level of said jet, the airflow Swirl Number (S') which is a parameter that quantifies the recirculating zone's intensity, and the ratio length/diameter (L/D) of the primary chamber, which characterizes the spatial availability for mixing reagents in the primary combustion zone. The influence of the Reynolds number, to a given swirl number and L/D ratio has been observed to vary through changes in diameter in the natural gas injection nozzle. Diameters of 2.35mm (Re=50,000), 3.20 mm (Re=40,000) and 7.8 mm (Re=15.000). were employed. The Swirl number was modified by altering the angle between swirler blades and the influence of L/D ratio was observed by changing the L length of the primary chamber (ALMEIDA, 2007).

To the simulation it was opted to build a tube in the same diameter of the primary chamber, but with a length L_d 10 cm. this tube has the function of housing the swirler and the fuel injection nozzle, as well as allowing initial development of air currents inserted into the chamber. The figure 2 shows all of the geometrical references. Models are grouped in five different configurations considering the three dimensionless numbers referring to the chamber geometry, that is, an injection nozzle with 2.35 mm will be represented by Re = 50,000, the 10 cm primary chamber will be represented by L/D = 1 and lastly, the 50° swirler angle will be represented by S' = 1.06.

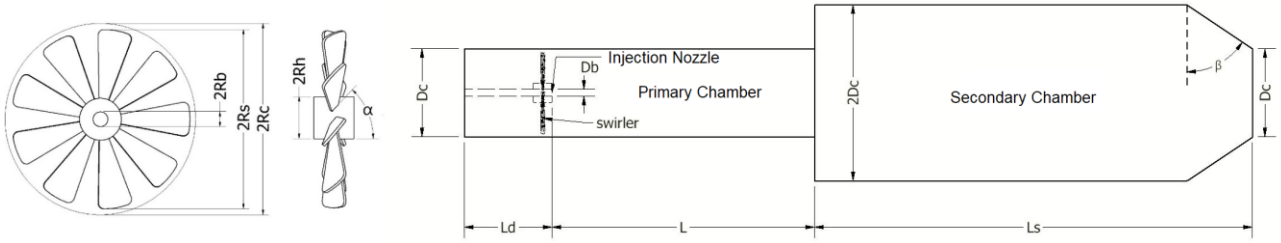

Figure 2. Swirler geometry (left) and studied chamber (right)
Adapted from Almeida (2007)

Swirlers appear as a form of stabilizing the flame and easing instabilities through homogenization of mixture due to the existence of recirculating zones. The swirler utilized in this work is similar to the one used by Almeida (2007). This device is comprised of 9 straight blades with thickness of T = 1.4 mm, a maximum diameter of D_s = 94mm, and the axis on with the blades were mounted upon has a diameter of D_h = 22mm. At the swirler center lies the fuel injection nozzle with diameter D_b. As discussed previously, a swirler causes recirculation zones to be generated, which in turn represents turbulence described by a dimensionless number named Swirl Number, S', defined by Couto *et al.* (1995) as:.

$$S' = \frac{S_s'}{(1+M_r)} \tag{1}$$

where S_s' and M_r are given, respectively as:

$$S_s' = \frac{G\phi}{(R_c - R_h)\cdot G_x'} \tag{2}$$

$$M_r = \frac{\left(\rho_{ar} / \dot{m}_{ar}^2\right)\cdot\left(\dot{m}_{comb}^2 / \rho_{comb}\right)\cdot(R_c^2 - R_h^2)}{R_b^2} \tag{3}$$

where ρ and $\dot{m}$ represent the specific mass and mass flow from the reaction components with indexes indicating their origin (air or fuel) Furthermore, the ratio $G\phi/G_x'$ is obtained by:

$$\frac{G\phi}{G_x^{'}} = \frac{2\cdot(CB)\cdot(\tan\alpha)\cdot(R_s^3 - R_h^3)}{3\cdot(R_c^2 - R_h^2)} \tag{4}$$

in which *CB* is the blockage coefficient and α is the swirler blade angle:

$$CB = \frac{1}{1-\sigma} \tag{5}$$

$$\sigma = \frac{(A_s - A_{ef})}{(A_{s,c} - A_s)} \tag{6}$$

where $A_{s,c}$ is the area between the swirler and the chamber walls; A_s is the circular area occupied by the swirler; and A_{sf}, obtained below, is the swirlers area of effective flow.

$$A_{ef} = 2\cdot(R_s - R_h)\cdot(K - 2T)\cdot\cos\alpha \tag{7}$$

So as to *K* corresponds to:

$$K = \cos(\pi/2Z)\cdot[R_s\cdot sen(\pi/Z) + R_h\cdot\tan(\pi/Z)] \tag{8}$$

Two airflows were employed in this work. Those would be the primary airflow that consists in air that was admitted in the primary chamber (in the experimental build such airflow is provided by air blowers with maximum mass flow rate of 100 g/s, being the simulations realized using mass flow as shown in table 1), and the secondary airflow consists in the air injected by the fuel nozzle (in the build, natural gas is employed with a constant mass flow rate of 1 g/s, being substituted here by a secondary airflow, characterizing as such, a cold simulation). The flow velocity of the first air flow (primary airflow) is given by the mass air-flow admission from the primary chamber $\dot{m}_{ar}$, hence the mass air-flow rate expression is applied in the area between the primary chamber's diameter D_c and the diameter of the injection nozzle D_b through equation (1). On its turn, the second air current velocity (secondary airflow), is based on the fuel jet Re (Re_{comb}). As such, it is assumed that such current holds the same Reynolds number as the fuel jet form the injection nozzle, mathematically:

$$V_{ar,1} = \frac{4\dot{m}_{ar}}{\pi\rho_{ar}\left(D_c^2 - D_b^2\right)} \tag{9}$$

$$V_{ar,2} = \frac{\mu_{ar}\,\mathrm{Re}_{comb}}{\rho_{ar}D_b} \tag{10}$$

where ρ_{comb}, ρ_{ar}, *and* μ_{ar} holding values of respectively 0.76226 kg/m^3, 1.08526 kg/m^3 and $1.04\cdot10^{-5}$ Pa·s according to the experimental model set by Almeida (2007).

The simulation configurations in table 1 were chosen based on the oscillation amplitude results of combustion instabilities, as shown in fig. 3, in which Almeida (2007) presented the most unstable condition with pressure amplitude of 11.93 and the less unstable condition with pressure amplitude of 0.30 mBar. It is noticed that the highest pressure peak is associated with a relatively low swirl number (S' = 1.06), a high Reynolds number (Re = 50,000) and smaller Length/Diameter ratio (L/D = 1), while the model with the lowest pressure peak shows high a swirl number (S' = 34.4), low Reynolds number (Re = 15,000) and higher Length/Diameter ratio (L/D = 3). Therefore, the five configurations chosen by this simulation are comprised of those two extreme models, as well as three intermediate ones.

Table 1. Configuration of Models for Simulation.

Models	L/D	Re	S'	m_{ar}(g/s)
1	3	15.000	34,4	88,09
2	3	50.000	1,06	44,89
3	1	50.000	34,4	88,09
4	1	15.000	1,06	71,79
5	1	50.000	1,06	41,81

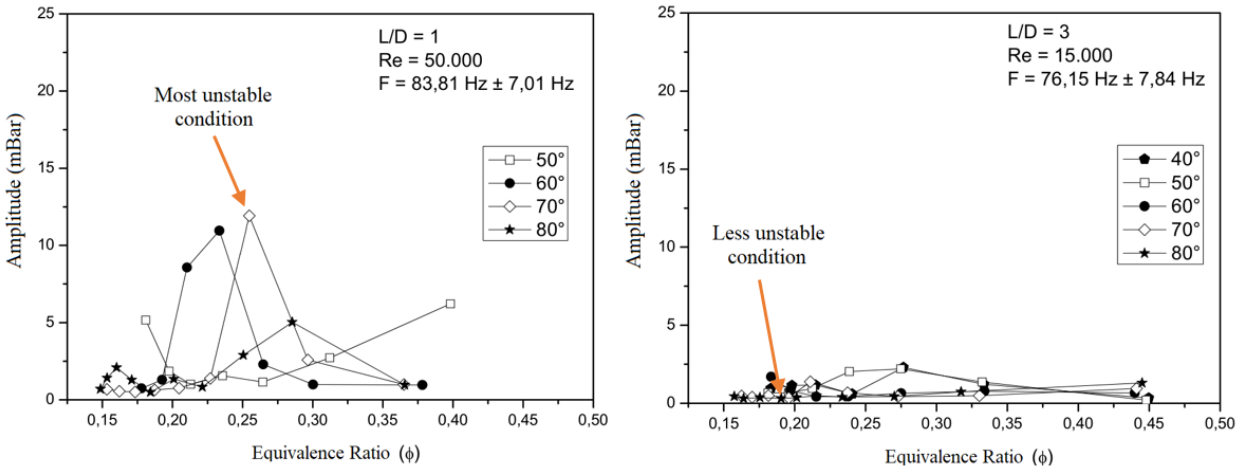

Figure 3. Comparison between configurations with greater and lesser amplitude of oscillation
Available from Almeida (2007)

The CAD models were drawn in *Autodesk*^{TM} 3D modelling software, *Inventor*. The choice comes from the low minimum requirements needed by the software when compared to other similar softwares in the market, as well as being already well-stablished software in the field. The numerical simulation *per se* occurred in ANSYS CFX package. This choice comes from its precision and reliability as also well-established software. After obtaining the CAD models those are exported in **.jgs* format in order to facilitate identification during it importing process in the CFX package. After importing the models, a tetragonal mesh was built off them, since such type of mesh can be easily adapted to multiple types of geometry, such as small curves in the swirler. The mesh has in average 367000 nodes and 260000 skewness elements (0, meaning the element is perfect and 1 meaning the element is completely deformed) with maximum of 0.97 and minimum of .29.

Brewster *et al* (1999), while compiling various works related to gas turbine combustor simulation noticed the κ-ε method is the most employed to solve the many problems and geometries analyzed. More recent works like Torkzadeh *et al* (2016) report the use of models such as κ-ε, κ-ω and SST as well in simulations of combustion chambers using swirlers as flame anchors. Hence, in the present work it was realized a numerical solution through technique STT (Sheer Stress Transport), based on previously cited works. Lastly the stopping criteria for iterations consists in a RMS error smaller than 1×10^{-4} or 300 iterations

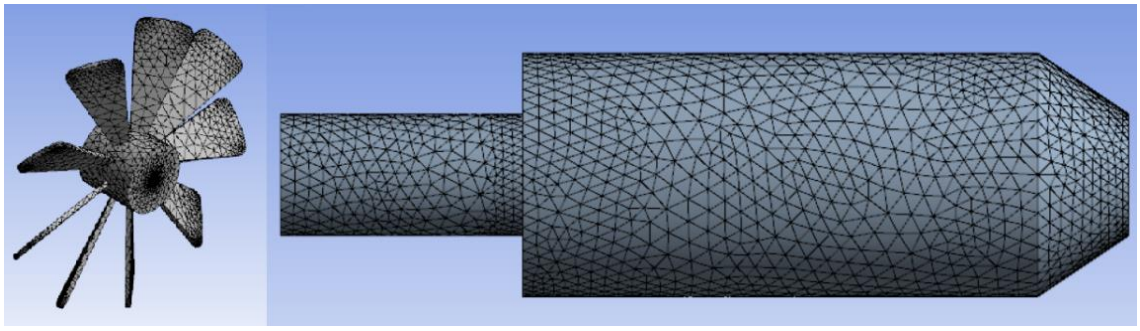

Figura 4. Mesh Used in Simulation.

3. RESULTS

In this section, the obtained results are shown as well as their descriptions and discussions. Simulations were realized in order to analyze, numerically, the influence of operational parameters, notably of swirl number, in a gas turbine combustion chamber geometry aiming to better comprehend formed recirculation zones (flow field) as well as their influence in combustion instabilities. The analysis has as starting point the use of results already obtained experimentally by Almeida (2007, 2011). The simulation configurations listed in tab. 1 where chosen based on figure 3. The first and the last represent, the configurations which yielded the highest and lowest oscillation amplitude, respectively, during experimental execution by Almeida (2007). The remaining are of comparative character; whose function is to demonstrate the influence of each dimensionless on the flow pattern.

Initially the influence of different L/D ratios over the flow field are compared, maintaining a swirl number of approximately S'≈1.06 (swirler blade inclination angle of 50º) and Re_{comb} = 50000.

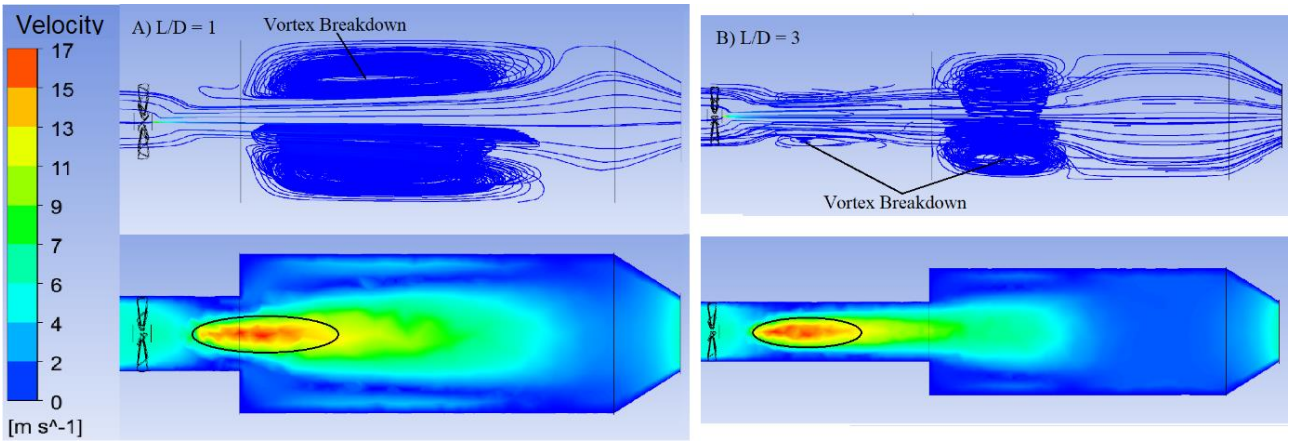

Figure 5. Influence of the L/D ratio on the flow.

Figure 5 shows high velocity through a red band that lies at the section between the primary chamber's exit and the secondary chamber's entry (5A) and inside the primary chamber (5B), evidencing that there is no significant changes in the flow field maximum velocity, even by increasing L/D ratio from 1 to 3. It is worth noting however that doing so reduces local velocity in the secondary chamber. This happens due to the increase in length that the primary-secondary air mixture must move through. Besides that, fig. 5B shows the occurrence of *vortex breakdown* within the primary zone. This presence makes itself troublesome to combustion-related applications because it induces, according to Benim and Syed (2014), the occurrence of *flashback* (propagation in the opposite direction of the flame), since this vortex breakdown drags the flame closer to the injection nozzle.

Figure 6 shows the influence Reynolds number alteration over the recirculation structure formed in the secondary region through the change from Re = 50000 (fig. 6A) to Re=15000 (Figure 6B). In this circumstances L/D ratio is kept at 1 and The Swirl Number is kept at around S' = 1.06. The change in the flow field is easily identified by the disappearance of the red band. It is realized that this reduction on Reynolds number allows for the extension of the recirculation zone towards the secondary chamber's exit, as to allow a higher contact area and interaction between air from primary and secondary chambers. As such, it becomes evident that a high Reynolds number deforms and reduces the size of the recirculation zone due to the velocity gradient between the primary chamber's intake air and the secondary air expelled by the fuel injection nozzle.

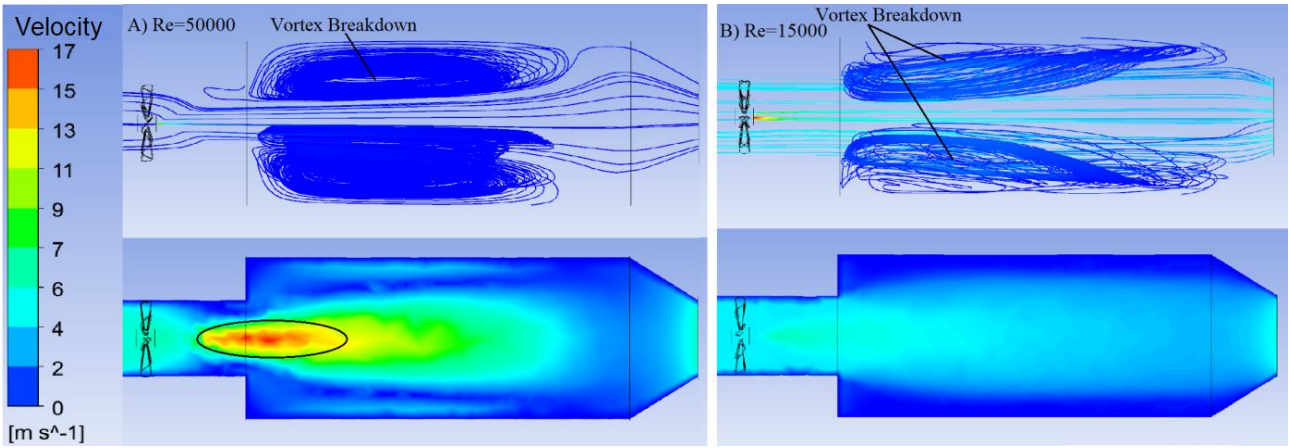

Figure 6. Reynolds number's influence over the flow.

The influence of the swirl number over recirculation zones is exhibited in Figure 7. To this end, the swirl number varies from S' = 1.06 (fig. 7A) to 34.4 (fig. 7B), while maintaining constant L/D = 1 and Re = 50000.

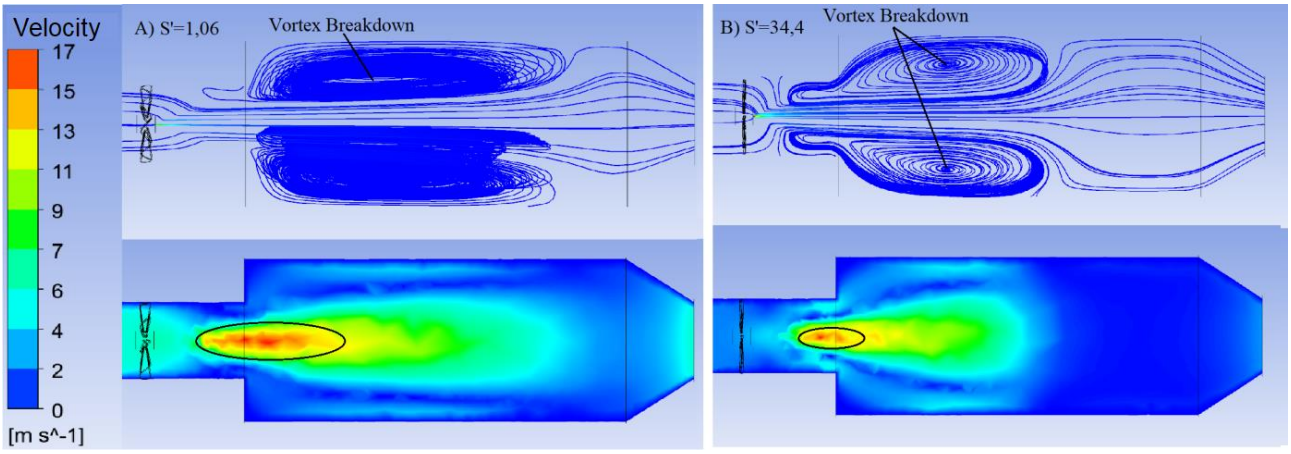

Figure 7. Swirl number's influence over the flow.

It has been noticed that increasing the swirl number by increasing the swirler blades angle, causes shrinking in the high velocity region at the primary chamber's exit through the diminishing of the red band, resulting on a considerable reduction of the velocity field in the secondary chamber's interior (smaller green and cyan zones) as well as generation of highly well-defined and symmetrical recirculation zones. Such phenomenon coincides with Gupta *et al.* (1984), in regards to axial velocity being reduced in detriment of tangential velocity due to the increase in the swirler blades's angle. Consequentially, the mixture with the highest tangential velocity will show a higher centrifugal force and in turn, higher adherence to the chamber's wall, and once it leaves the primary zone and suffer expansion when entering the secondary chamber, produces an increase in the size of the recirculation zone due to the higher pressure gradient between the geometric center of the chamber and the air flowing closer to the combustor walls.

Figure 8 presents a comparison between the behaviors of recirculation structures for operational conditions that lead to higher (Re=50,000, L/D=1 and *S'*=1.06) and lower (Re=15000, L/D=3 and *S'*=33.5) amplitude obtained during experiments performed by Almeida (2007). In this condition, the flow does not present any high velocity zone, the recirculation structures are localized entirely in the secondary chamber, and they are characterized by large, elongated shape, which has higher intensity, as to stretch almost completely over the secondary chamber's region.

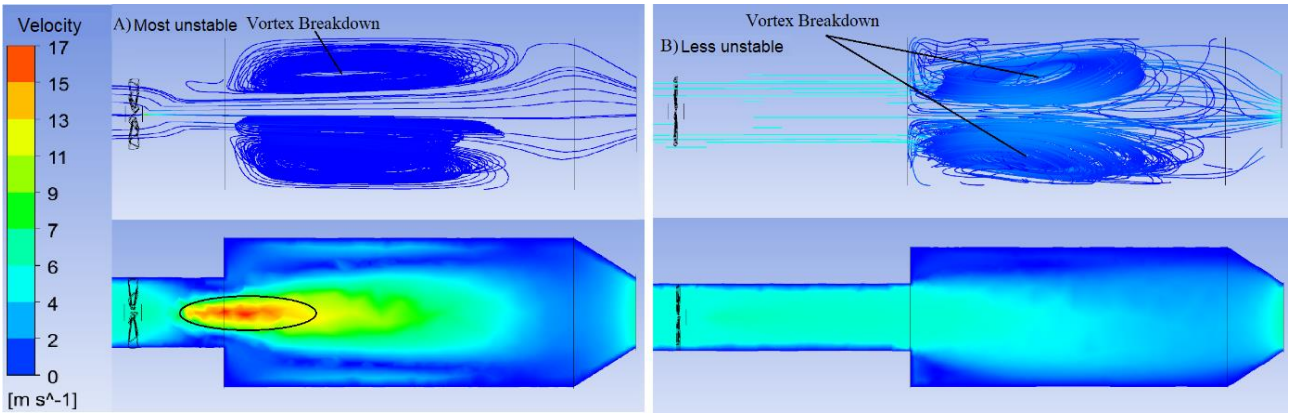

Figure 8. Comparison between the configuration with higher (a) and lower (b) pressure ranges.

Almeida (2007) reports that the increase in the swirler blade angle from S'=50º to S'=80º eases the oscillations due to the increase in the homogenization level of the mixture. Simulation-wise, this increase in homogenization is confirmed as the result of fig. 7, where can be noticed an increase in size and quality of the recirculating zone in the secondary chamber as well as a decrease in flow velocity at the primary chamber's exit, which in turn provides higher stability to flame anchoring during combustion. In addition, Almeida (2007) attributes the large pressure amplitudes to the high Reynolds number from the fuel jet (in this case the secondary air current), hence the high velocity in the secondary chamber. When Re = 50,000 is employed, oscillation amplitudes reach 13 mBar, as seen in 3. The high velocity in the primary chamber tends to destroy the recirculation zone formed in this region. This can be confirmed by the elongated and better defined recirculation pattern towards the combustor's exit created in Fig. 6B when compared to Figure 6A.

In respect to chambers (Fig. 5), it has been noticed that a ratio of L/D = 3 leads to the formation of a well-defined, elongated and uniform recirculation zone. Such behavior does not occur clearly in the L/D = 1 configuration, because it

is understood there was not enough distance to move through (longer length of the primary chamber) in order to generate the decrease in intensity of the vortex generated by the swirler, as well as the intensity of said vortex is not sufficient to form a well-defined CTRZ.

In respect to Fig. 8, Almeida (2007) it has been noticed that the operational condition with L/D = 3 provides higher stability (that is, lower pressure amplitude) when compared to other models. In this condition, there is a tendency of damping the oscillations. However, besides increasing L/D from 1 to 3 and the swirl number from 1.06 to 34.4, the Reynolds number still presents itself as the defining factor to instability generation, since Re = 50,000 shows pressure amplitude close to 13 mBar while to Re = 15,000 oscillations inferior to 5 mBar are obtained, according to Figure 6.

Lastly, it has been noticed that as much as in the numerical simulation as in the experimental data from Almeida (2007) a high Reynolds number from the injection nozzle, can destroy or hamper the formation of recirculating zones due to their high velocity. In conjunction, it has been noticed that not necessarily every s*wirl* number above 0.6 is capable of generating flows turbulent enough to produce well defined and stable recirculation zones.

Additionally, regarding combustion, the *flashback* caused in the configurations with high Reynolds and low *swirl*, can cause combustion instabilities to appear. Furthermore, a badly formed or placed recirculation zone my lead hinder the mix between combustion byproducts and mix gases (fuel and air from the injection nozzle) to be ignited, leading to efficiency loss and/or pollutant generation.

Besides the already explored parameters, Almeida (2011) suggests increasing the secondary chamber's diameter in order to attenuate of instabilities, since a higher diameter intensifies the recirculation zones as to favor greater mixture homogeny, and consequentially less oscillation in energy liberation.

4. CONCLUSIONS

The present work analyzed, numerically, the experimental results obtained by Almeida (2007) in a laboratorial scale combustor for gas turbine application. From the evaluated parameters in the simulation (S', L/D, Re), it has been noticed that high S' (34.3) allows for the formation of a larger and more elongated recirculation structure when compared to a relatively low S' (1.06) this recirculation zone, in turn allows for a higher interaction between secondary and primary airflows, something that in terms of combustion, provides a better mixture between the hot combustion gases and the reagents (air and fuel), facilitating ignition and certain uniformity of heat release, thus reducing instabilities.

Therefore, not necessarily every S' number above 0.6 will form uniform, large and well defined recirculation zones. Note that CTRZ forms independently of the swirl number of the airflow, hence only vortex breakdown and precessing vortex core will show more visibility. These structures appear due to how the secondary air flow velocity carries the primary flow due to is viscosity and the pressure gradient between the two flows. As such, the higher the Reynolds number in this air flow (and consequentially the higher velocity), the farther the recirculation zone will be located from the chamber's geometric center, and this secondary chamber zone's uniformity will be smaller. Hence, based on the performed simulations, in order to obtain a stable flow field, the recirculating zones must be well defined and uniform, and the employed Re_{comb} must be low enough to prevent deformation of destruction of said zones, as to in a combustion process, instabilities are to be minimized. A higher L/D ration also favors the preservation of formed recirculation zones.

In addition, results analysis also shows that an increase of L/D from 1 to 3 acts as a complement in the formation of recirculation zones, since their function is to reduce the flow velocity with the primary chamber's increase in length. A high Reynolds number (Re = 50,000) in turn, deforms and destroys recirculation zones, as well as produces high flow velocitys. The presented simulations make evident that conclusions about the creation of high pressure amplitudes in a flow field is not an easy task, since there are distinct and complex processes that are inherent to such phenomena. However, it was possible to verify how the parameters here in studied influence the appearing of pressure amplitudes. In general, it is recommended a high swirl number (S' = 34.4) a larger length/diameter ratio (L/D = 3) and a low Reynolds number (Re=50,000) to stably operate and attenuate the presence of instabilities.

5. ACKNOWLEDGEMENTS

Thanks the Federal University of Maranhao (UFMA) for providing the necessary structure for the development of this work.

6. REFERENCES

ALMEIDA, Dener Silva de. *Análise de Instabilidades Termoacústicas e Emissões Poluentes em Câmaras de Combustão do Tipo Duplo-Estágio para Aplicação em Turbinas a Gás*. 2011. 193 f. Tese (Doutorado) - Instituto Tecnológico da Aeronáutica, São José dos Campos.

ALMEIDA, Dener Silva de. *Detecção de Instabilidades Termoacústicas em Câmaras de Combustão do Tipo RQL para Aplicação em Turbinas a Gás*. 2007. 123 f. Dissertação (Mestrado) - Instituto Tecnológico da Aeronáutica, São José dos Campos.

BREWSTER, B.Scott et al. Modeling of lean premixed combustion in stationary gas turbines. *Progress In Energy And Combustion Science*, [S.l.], v. 25, n. 4, p. 353-385, ago. 1999.

GUPTA, A.k. *et al*. *Swirl Flows*. Tunbridge Wells: Abacus Press, 1984. 475 p.

HUANG, Ying; YANG, Vigor. Dynamics and stability of lean-premixed swirl-stabilized combustion. *Progress In Energy And Combustion Science*, [S.l.], v. 35, n. 4, p. 293-364, ago. 2009.

LEFEBVRE, A. H.; BALLAL, D. R.. *Gas Turbine Combustion*: Alternative Fuels and Emissions. 3. ed. Londres: Taylor & Francis Group, 2010. 557 f.

LEIBOVICH, S. The Structure of Vortex Breakdown. *Annual Review of Fluid Mechanics*, [S.l], v. 10, n. 1, p. 221-246, 1978.

LIEUWEN, Timothy C.. Static and Dynamic Combustion Stability. In: SMITH, Lance et al (Org.). *The Gas Turbine Handbook.* [S.l.]: [s.n.], 2006. Cap. 3.1.1. p. 197-2.

LIEUWEN, Timothy C; YANG, Vigor (ed.). *Combustion Instabilities in Gas Turbine Engines*: Operational Experience, Fundamental Mechanisms, and Modeling. [S.l]: American Institute Of Aeronautics And Astronautics, 2005. 729 p.

RICHARDS, G. A.; JANUS, M. C.. Characterization of Oscillations During Premix Gas Turbine Combustion. *Journal of Engineering For Gas Turbines and Power*, [S.l.], v. 120, n. 2, p. 294-302, 1 abr. 1998.

SUNG, Hong-Gye. Combustion dynamics in a model lean-premixed gas turbine with a swirl stabilized injector. *Journal of Mechanical Science and Technology*, [S.l.], v. 21, n. 3, p. 495-504, mar. 2007.

TORKZADEH, M.M. et al. An investigation of air-swirl design criteria for gas turbine combustors through a multi-objective CFD optimization. *Fuel*, [S.l.], v. 186, p. 734-749, dez. 2016.

7. RESPONSIBILITY NOTICE

The authors are the only responsible for the printed material included in this paper.